



**INORGANIC  
CHEMISTRY**  
FRONTIERS

## Highly active copper catalyst obtained through rapid MOF decomposition

Journal:	<i>Inorganic Chemistry Frontiers</i>
Manuscript ID	QI-RES-11-2018-001217.R1
Article Type:	Research Article
Date Submitted by the Author:	12-Dec-2018
Complete List of Authors:	Nguyen-Sorenson, Anh ; Brigham Young University, Chemistry and Biochemistry Anderson, Clifton; Brigham Young University, Chemistry and Biochemistry Balijepallic, S.; Brigham Young University, Chemistry and Biochemistry McDonald, Kyle; University of Michigan, Chemistry Matzger, Adam; University of Michigan, Chemistry Stowers, Kara; Brigham Young University, Chemistry and Biochemistry

SCHOLARONE™  
Manuscripts



Journal Name

ARTICLE

## Highly active copper catalyst obtained through rapid MOF decomposition

Received 00th January 20xx,  
Accepted 00th January 20xx

Anh H. T. Nguyen-Sorenson,<sup>a</sup> Clifton M. Anderson,<sup>a</sup> Santosh K. Balijepalli,<sup>a</sup> Kyle A. McDonald,<sup>b</sup> Adam J. Matzger,<sup>b</sup> and Kara J. Stowers<sup>\*a</sup>

DOI: 10.1039/x0xx00000x

www.rsc.org/

**A decomposed copper based metal-organic framework containing amorphous Cu species was found to be a highly reactive carbon supported catalyst (a-Cu@C). This catalyst is active for reduction, oxidation, and N-arylation reactions without further tuning or optimization. Higher catalyst turnover numbers for each of these transformations are obtained when comparing a-Cu@C activity to similar Cu-based materials.**

### Introduction

Heterogeneous catalysis is critical for both the energy and chemical industries.<sup>1</sup> The innovation of robust materials that have long-lived active sites can decrease energy costs and minimize catalyst regeneration costs. It is typical to design a catalyst optimized for one reaction. However, in order to achieve optimal activity for different reactions, this often requires a different support material, active site, or additional promoters. There is need for an easily synthesized, recyclable, and general catalyst that can be used for multiple transformations without further pretreatments.

Recently, metal-organic frameworks (MOFs) have attracted much attention as catalysts due to their unique architectures, large surface area, flexible pore structure and remarkable variety of functional group selection.<sup>2</sup> While MOF-based catalysts are recyclable and reactive, some are susceptible to basic or acidic decomposition, sensitive to solvent choice, and can leach active metals into solution. Research into MOF catalysis is mainly driven towards expanding scope and efficiency; however, there is an increasing emphasis on using MOFs as both sacrificial templates and metal nanoparticle

precursors for the preparation of heterogeneous supported catalysts.

The decomposition of MOFs allows the design of catalytically active metal or metal oxide nanoparticles deposited on carbonaceous supports through thermolysis conditions.<sup>3</sup> Some have even used the decomposition of MOFs with other materials such as metal oxides, nanorod templates, and graphene itself to create hybrid materials used for catalysis.<sup>4</sup> These materials provide a template for smaller and more consistent metal nanoparticles compared to traditional approaches such as impregnation or vapor deposition. Moreover, they can yield catalysts that are stable and easily recycled. There have been a few cases of Cu-based catalysts derived from MOFs, with the majority of them derived from HKUST-1.<sup>5-7</sup> Each catalyst was decomposed and annealed at high temperatures prior to the reaction; Oxidation and reduction reactions have both proven feasible. For example, a catalyst system was used for aerobic benzyl alcohol oxidation,<sup>5</sup> while a different group reported on the reduction of 4-nitrophenol in the presence of NaBH<sub>4</sub>.<sup>6</sup> Recently, the synthesis and catalytic activity of a different Cu-based MOF, [Cu(pdc)]<sub>n</sub>, was pyrolyzed and the derived CuO nanoparticles were used for the synthesis of  $\alpha$ -aminonitriles.<sup>7</sup>

Compared to the HKUST-1 MOF-derived Cu-oxide/carbon nanocomposites reported, the high energy CuNbO-1 MOF from our previous report<sup>8</sup> offers a distinct precursor for a copper based material that has yet to be tested for any catalytic activity. CuNbO-1 can be transformed into a copper and anisotropic carbon nanocomposite (denoted as **a-Cu@C**) by a deflagration initiated at a much lower temperature (~250 °C) than conventional pyrolysis methods. Such a rapid process may be expected to reduce the effect of particle agglomeration that often occurs upon high temperature annealing. The resulting composite has highly dispersed copper species throughout the layers of an anisotropic carbon structure (Fig 1). Herein, we have included further characterizations on the nature of **a-Cu@C** and demonstrate its remarkable capability as a general heterogeneous catalyst

<sup>a</sup> Department of Chemistry and Biochemistry, Brigham Young University, Provo Utah, 84604, USA

<sup>b</sup> Department of Chemistry, University of Michigan, Ann Arbor, Michigan, 48109-1055, USA

\* All correspondence should be sent to [kstowers@chem.byu.edu](mailto:kstowers@chem.byu.edu).

Electronic Supplementary Information (ESI) available: Complete synthetic procedures and XPS spectra are included. See DOI: 10.1039/x0xx00000x

by comparison to oxidation and reduction reactions reported by others, and will also disclose activity for a novel N-arylation.

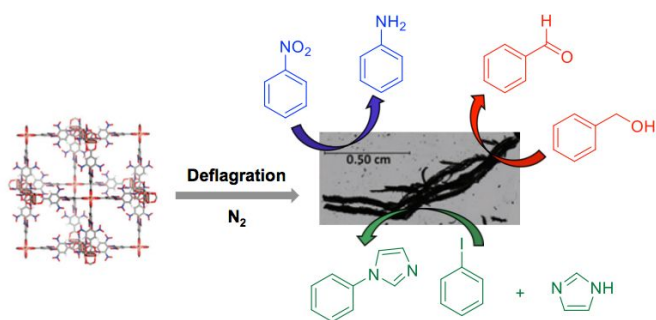


Figure 1. CuNbO-1 is decomposed to **a-Cu@C**, which can be used to catalyze alcohol oxidation, nitro-group reduction, and C-N bond formation.

## Experimental section

### Chemicals and Materials

All reagents and starting materials were purchased commercially from Sigma-Aldrich or Alfa-Aesar, and used as received without any further purification unless otherwise noted.

### Characterization

Transmission electron microscopy-energy dispersive X-ray spectroscopy (TEM-EDX) studies were performed on a Tecnai F20 TEM using an accelerating voltage of 200 kV. The electronic binding energy of the sample was examined by X-ray photoelectron spectroscopy (XPS) using a Surface Science SSX-100 XPS instrument (serviced by Service Physics, Bend, OR) with a monochromatic Al K $\alpha$  source (1486.7 eV) and a hemispherical analyzer. Narrow scans were recorded with a spot size of 500  $\mu\text{m}$   $\times$  500  $\mu\text{m}$ , resolution: 4 (nominal pass energy 100 eV), number of scans: 20, and step size of 0.065 eV. The Cu@C spectrum was referenced to the main C 1s peak in the narrow scan, which was taken at 284.5 eV. Peak fitting was performed using instrument software ('CASA XPS'). The curve-fitting of the Cu 2p $_{3/2}$ , C 1s, N 1s, and O 1s lines for Cu@C was employed Gaussian (70%)-Lorentzian (30%) peak-shapes, respectively (defined in CasaXPS as GL (30)). The Cu wt.% loading was determined by inductively coupled plasma mass spectrometry (ICP-MS) from Agilent Technologies (7800 ICP-MS) using argon and a collision cell filled with ultra-high-purity helium both from Airgas. The reaction products were also characterized by gas chromatography mass spectrometry (GC-MS) QP2010 SE from Shimadzu.

### Catalytic Alcohol Oxidation

Catalysts (0.05 equiv., 0.025 mmol) and TEMPO (0.05 equiv., 0.025 mmol) was added to a 25 mL round-bottom flask equipped with a magnetic stir bar. This flask was evacuated and charged with oxygen from a balloon. To this mixture, benzyl alcohol (1 equiv., 0.5 mmol) and NMI (0.2 equiv., 0.1 mmol) was added with 1 mL of acetonitrile. The mixture was stirred for 9 h at 70  $^{\circ}\text{C}$  under an O $_2$  environment. Once the

reaction was completed, toluene was used to dilute the reaction mixture for GC-MS analysis. A yield of the aldehyde product was determined by integration using an internal standard (biphenyl) in the GC-MS.

### Catalytic Reduction of Nitrobenzene

Typically, nitrobenzene (1 equiv., 1 mmol) and 3 mL of THF:H $_2$ O (1:2) solution were added into a 40 mL pressurized tube in sequence, followed by the addition of catalyst (0.05 equiv., 0.05 mmol) to the mixture. NaBH $_4$  (3 equiv., 3 mmol) was dissolved in 5 mL D.I. H $_2$ O and added dropwise to the reaction mixture under continuous stirring. The mixture was stirred for 2 h at 50  $^{\circ}\text{C}$ . Once the reaction was completed, it was cooled to room temperature followed by filtration. The filtrate was washed with CH $_2$ Cl $_2$ . The organic layer was washed with brine solution and D.I. H $_2$ O. Then, it was dried with anhydrous Na $_2$ SO $_4$  and filtered. The solvent was removed under vacuum. A yield of aniline product was determined by GC-MS.

### Catalytic N-arylation

A total of 1.0 mmol of iodobenzene, 1.2 mmol of imidazole, 2.0 mmol of KOH, and 1 mol% Cu@C catalyst were placed in a 25 mL round-bottom flask. Dimethyl sulfoxide (DMSO, 2 mL) was added in ambient air. The reaction mixture was rapidly heated to 110  $^{\circ}\text{C}$  in a sand bath and kept at this temperature for 24 h. After cooling to room temperature, the reaction mixture was analyzed by GC-MS after dilution with toluene.

## Results and discussion

The MOF-derived nanocomposite **a-Cu@C** was obtained by decomposition of CuNbO-1 as a precursor in a nitrogen atmosphere.<sup>8</sup> Previously, **a-Cu@C** was found to have unusual morphology with highly dispersed copper species; therefore, a further characterization of this material would elucidate the properties relevant to catalytic activity in oxidation and reduction reactions. This material was found to contain amorphous carbon based on the Raman spectrum with no long-range order, which was confirmed by transmission electron microscopy (TEM). The powder X-ray diffraction (PXRD) spectrum only showed a broad peak centered at diffraction angle of  $2\theta = 18.0^{\circ}$ , which is between the diffraction angles of pure graphite and graphene oxides. The Sherrer equation was used to calculate the thickness of the carbon material, which corresponds to the stacking of three carbon layers. *Notably, no diffraction patterns were observed for a nanoparticle copper species present on the carbon.* Scanning transmission electron microscopy (STEM) images of **a-Cu@C** further clarify the sizes of the copper sites. Bright features with irregular shape were observed throughout an amorphous carbon matrix with the distribution as shown in the box and whisker plot (Fig. 2). Analysis of the features in Fig. 2a shows a broad size distribution with a median size of 160 nm. The analysis of diffraction patterns from TEM data (Fig. 2b, inset), showed weak or absent lattice fringes adding additional evidence that there is little to no long-range order of the small

agglomerates. Additionally, the lack of a distinguishable

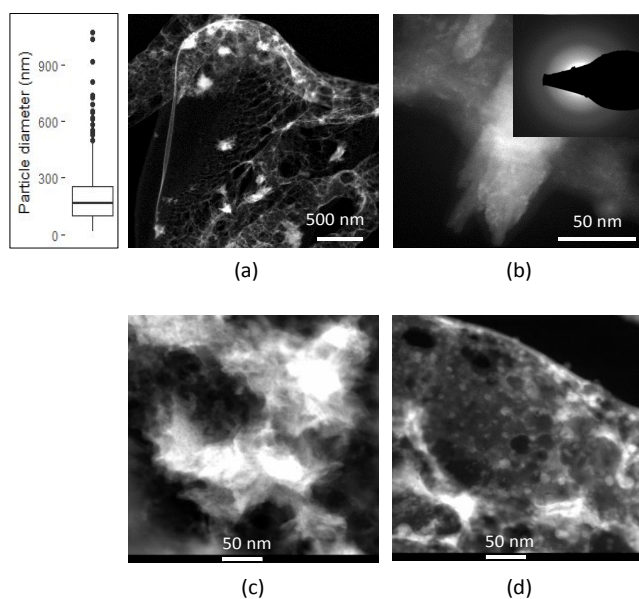


Figure 2. TEM images of **a-Cu@C** with statistical analysis of feature size; a) wide view of Cu features in anisotropic carbon matrix, b) magnification of **a-Cu@C** with inset STEM derived diffuse diffraction pattern, c) magnification of **a-Cu@C** with multiple layers of anisotropic carbon matrix, d) magnification of **a-Cu@C** showing carbon encapsulation.

copper in the sample is amorphous copper with crystallite sizes less than 3 nm. It is unclear whether the copper species in **a-Cu@C** are dispersed on or embedded within the carbon matrix as observed by Niu.<sup>6</sup> It is also possible that the 160 nm features in Fig. 2 consist of small copper nanoparticles close together but encapsulated in carbon, which was also seen for a cobalt MOF decomposition material reported by Diaz-Duran.<sup>9</sup> However, in the most magnified image (Fig. 2c and d), the Cu species are seen with carbon surrounding small bright features supporting a Cu encapsulation with some species embedded within the matrix.

X-ray photoelectron spectroscopy (XPS) was used to investigate the elemental composition and oxidation states of copper in the carbon matrix. The Cu 2p<sub>1/2</sub> and Cu 2p<sub>3/2</sub> peaks indicated the dominant oxidation state of Cu was ascribed to Cu<sup>0</sup>/Cu<sup>+</sup>, whereas the minor species was Cu<sup>2+</sup> (Fig. 3).<sup>10</sup> During the pyrolysis of CuNbO-1 MOF in N<sub>2</sub>, the organic ligands H<sub>2</sub>BPDC-(NO<sub>2</sub>)<sub>4</sub> are decomposed and carbonized, which can potentially lead to the reduction of Cu<sup>2+</sup> to produce Cu and/or Cu<sub>2</sub>O species.<sup>11</sup> The C1s, O1s, and N1s XPS spectra are consistent with a majority of sp<sup>2</sup>-carbon with graphitic nature,<sup>12</sup> the presence of copper oxides,<sup>12</sup> C–OH and C=O groups on the surface of carbon matrix and Cu coordinated N, graphitic N, and oxidized N.<sup>14</sup>

Metal nanoparticles, especially copper, on graphite-based supports can easily reduce under XPS analysis.<sup>15</sup> However, compared to the other MOF-derived catalysts, the oxidation states are similar. There is no Cu<sup>2+</sup> reported in one of the HKUST-1 catalysts, while the other suggests that there may be a Cu<sup>2+</sup> oxidation state. This is in agreement with what we

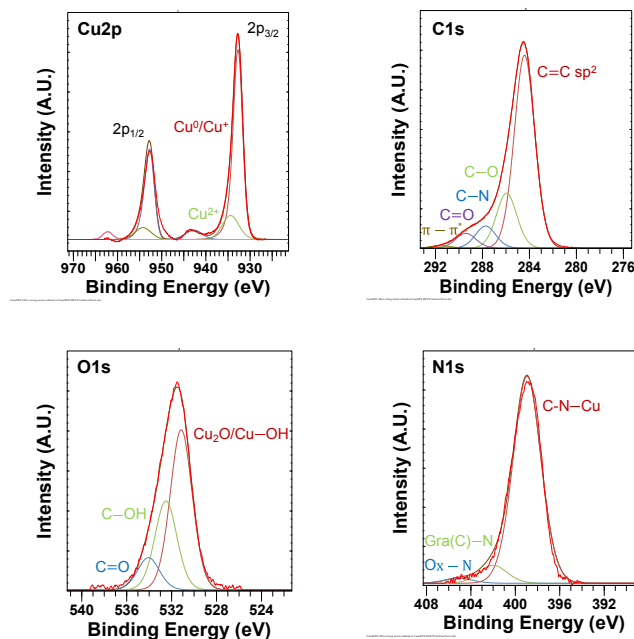


Figure 3. XPS spectra of **a-Cu@C**.

observe. Due to the pre-treatment of these catalysts after derivation from the MOF, the particle sizes are quite different (Table 1). The annealing temperatures of the HKUST-1 catalysts are around 600–800 °C held for at least 4–6 hours.<sup>5,6</sup> From their TEM images, the particles are calculated at 40–58 nm in size. *This is noticeably different from the CuNbO-1 derived catalyst, which has no detectable crystalline copper species as judged by the XRD - but is agglomerated into nanoscale aggregates visible in TEM.*

One benchmark for characterizing catalyst activity is through the turnover number, or the moles of converted substrate divided by moles of catalyst used. For these catalysts that have low surface area and may be encapsulated, much of the Cu species may be unused. Therefore, this is a low estimate as the number would be higher if only the active Cu species were used in the calculation. We have used this measure for comparing catalyst activity within similar reaction conditions. The first class of reactions that we used to benchmark the activity of **a-Cu@C** was oxidation. In the fine chemical industry, the selective conversion of alcohols to the corresponding aldehydes is an important principal step prior to introducing further complexity.<sup>16</sup> The advantages of this reaction are the use of molecular oxygen as an environmentally friendly oxidant and mild reaction conditions. Many different coinage metal-based catalysts have been used for aerobic oxidation with TEMPO and molecular oxygen (Table S1). An HKUST-1 MOF-derived catalyst reported from Kim's group has been used for the aerobic oxidation of benzyl alcohol<sup>5</sup>; therefore, these conditions and procedure were used

Table 1. Comparison of physical properties between Cu-C composites obtained through MOF-decomposition.

Entry	XPS	TEM (nm)	Ref.
1	Cu <sup>0</sup> /Cu <sup>+</sup> /Cu <sup>2+</sup>	< 3	This work

2	Cu <sup>0</sup> /Cu <sup>+</sup>	57.6	5
3	Cu <sup>0</sup> /Cu <sup>+</sup> /Cu <sup>2+</sup>	40	6

Table 2. Cu-catalyzed aerobic oxidation of benzyl alcohol

Entry	Catalyst (mol%)	Yield <sup>b</sup> (%)	TON <sup>c</sup>
1 <sup>*</sup>	Cu-C (5.0)	94	18.8
2	<b>a-Cu@C</b> (5.0)	100	20
3	<b>a-Cu@C</b> (1.0)	100	100
4	<b>a-Cu@C</b> (0.5)	89	178

\* See reference 5. <sup>a</sup> Reaction conditions: benzyl alcohol (1 mmol), TEMPO (5 mol% to benzyl alcohol), NMI (0.2 equiv.), catalyst (0.5 – 5.0 mol% to benzyl alcohol), and CH<sub>3</sub>CN (1 mL) under O<sub>2</sub> balloon, 70 °C, 9 h. <sup>b</sup> Determined by GC-MS using biphenyl as internal standard. <sup>c</sup> Turnover number (TON) = [moles of converted substrate (benzyl alcohol)] × (moles of Cu)<sup>-1</sup>.

in order to compare the activity of **a-Cu@C** (Table 2). This reaction was conducted under molecular oxygen atmosphere at 70 °C in the presence of 2,2,6,6-tetramethyl-1-piperidinyloxy (TEMPO) and N-methyl imidazole (NMI) along with **a-Cu@C**. With 5 mol% catalyst loading, Kim's material converted benzyl alcohol to 94% yield<sup>5</sup> of desired product, benzaldehyde, resulting in 18.8 TON (entry 1). Under these mild reaction conditions, the selectivity for benzaldehyde was excellent and no traces of benzoic acid were detected. With a catalyst loading of 5 mol% **a-Cu@C**, benzyl alcohol was successfully converted to benzaldehyde in excellent yield, 100 % (entry 2). The activity of **a-Cu@C** was still as efficient with 1 mol% of catalyst resulting in 100 TON (entry 3). However, when decreasing the catalyst loading to 0.5 mol%, the conversion of benzyl alcohol was reduced (entry 4); but the catalyst was still productive resulting in 178 TON. Comparing **a-Cu@C** catalyst activity between different amounts of catalyst, the TON increases by 9 times when decreasing the 5 mol% loading to 0.5 mol% loading.

We next set out to benchmark the activity for reduction reactions, which are a typical application of coinage metal-based materials. In general, the reduction of nitrobenzene to aniline has been used as a model reaction to evaluate the catalytic performance of Cu-based nanoparticles (Table S2). Previously, Niu and coworkers used the HKUST-1-derived, Cu-C composite, for the reduction of 4-nitrophenol in the presence of NaBH<sub>4</sub>.<sup>6</sup> While the catalyst reported higher catalytic rates than a Au-based catalyst for this reaction (Table 3, entry 1); it is difficult to determine the activity due to a high catalyst loading (50 mol%). Other reports have shown that 10 mol% commercial CuO could be used to obtain 7.9 TON, while synthesized Cu NPs performed slightly better with 9.8 TON (Table 3, entries 2 and 3 respectively).<sup>17</sup> These conditions were selected as a better comparison for testing the activity of the **a-Cu@C** catalyst. Using 10 mol% of **a-Cu@C**, a slightly lower

conversion of nitrobenzene reduction to aniline was obtained (entry 4). Although this reaction can lead to coupling products such as hydrazines and hydroxylamines, none of these side products were detected under these reaction conditions.

Table 3. Cu-catalyzed reduction of nitrobenzene with NaBH<sub>4</sub>

Entry	Catalyst (mol%)	Time (h)	Yield <sup>b</sup> (%)	TON <sup>c</sup>
1 <sup>*</sup>	Cu-C (50.0)	< 1 min	100	2
2 <sup>**</sup>	CuO (10.0)	2	79	7.9
3 <sup>**</sup>	Cu NPs (10.0)	2	98	9.8
4	<b>a-Cu@C</b> (10.0)	2	87	8.7
5	<b>a-Cu@C</b> (5.0)	2	67.5	13.5
6	<b>a-Cu@C</b> (5.0)	4	75	15

\* See reference 6. \*\* See reference 17. <sup>a</sup> Reaction conditions: nitrobenzene (1 mmol), NaBH<sub>4</sub> (3 equiv. to nitrobenzene), catalyst (5.0 – 50.0 mol% to nitrobenzene), and THF/H<sub>2</sub>O (1:2, 3 mL), 50 °C, 2-4 h. <sup>b</sup> Determined by GC-MS using biphenyl as internal standard. <sup>c</sup> Turnover number (TON) = [moles of converted substrate (nitrobenzene)] × (moles of Cu)<sup>-1</sup>.

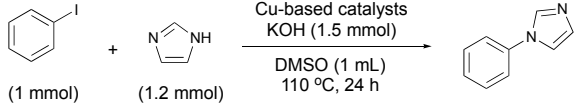
Decreasing the **a-Cu@C** catalyst loading by half yields even lower conversion; but it exceeds the TON of previously used Cu based catalysts (entry 5). Higher activity can be obtained using a longer reaction time (entry 6), but this only slightly increases the TON. Due to the carbon matrix and agglomeration of the **a-Cu@C**, it could be that some Cu<sup>2+</sup> species are encapsulated within the matrix and cannot be reduced. This would leave unreduced active sites that cannot be further optimized for reduction reactions.

With oxidation and reduction reactions benchmarked for the activity of **a-Cu@C** compared to other MOF-derived Cu-C composites, we next chose to study the C-N bond formation between iodobenzene and imidazole as a new reaction for MOF-derived carbon-based materials. These copper-catalyzed C-N bond formations are widely used in academia and industry for the synthesis of natural products, pharmaceuticals and other biologically active materials.<sup>18</sup> Many different Cu-based catalysts have been used for N-arylation including MOFs (Table S3). Under basic conditions with KOH the parent Cu-NbO MOF does not stay intact and all Cu activity comes from Cu in solution. This reaction was carried out at 110 °C, using iodobenzene and imidazole as model substrates in the presence of KOH, under ambient air which is the most frequently reported conditions for this reaction in order to compare with other Cu-based catalysts (Table 4). The activity of the **a-Cu@C** catalyst with only 1.0 mol% catalyst loading and 1.5 equivalents of KOH at 110 °C, afforded 88% yield of 1-phenyl-imidazole product (entry 1). The only side products detected for N-arylation under these reaction conditions are iodobenzene hydrolysis to phenol upon reaction work up. The activity of **a-Cu@C** remained high after decreasing the catalyst to 0.5 mol% resulting to 168 TON (entry 2). Finally, decreasing

the catalyst loading to 0.25 mol% reduced the yield of 1-phenyl-imidazole product by 10%, resulting in 74% yield (entry 3). While MOF-derived Cu based catalysts have not been used for this reaction, Cu-based nanoparticles have. Recently, Dabiri

states and maximizing surface area are underway. The rapid decomposition of this highly energetic MOF is a promising and powerful strategy for preparing a stable heterogeneous catalyst with high activity.

Table 4. Cu-catalyzed N-arylation of imidazole using iodobenzene\*



Entry	Catalyst (mol%)	Yield <sup>b</sup> (%)	TON <sup>c</sup>
1	<b>a-Cu@C</b> (1.0)	88	88
2	<b>a-Cu@C</b> (0.5)	84	168
3	<b>a-Cu@C</b> (0.25)	74	296
4*	Cu NPs-MCN (2.5)	98	39.2
5**	Fe <sub>3</sub> O <sub>4</sub> @SiO <sub>2</sub> /Salen-Cu(II) (0.4)	82	205

\*See reference 19. \*\* See reference 20. <sup>a</sup> Reaction conditions: iodobenzene (1 mmol), imidazole (1.2 mmol), catalyst (0.5 – 10.0 mol% to iodobenzene), KOH (1.5 mmol), DMSO (1 mL), 110 °C, 24 h. <sup>b</sup> Determined by GC-MS using biphenyl as internal standard. <sup>c</sup> Turnover number (TON) = [moles of converted substrate (iodobenzene)] × (moles of Cu)<sup>-1</sup>.

et al. has reported a new catalyst containing copper nanoparticles incorporated on a mesoporous carbon nitride for N-arylation of N-heterocycles.<sup>19</sup> With 2.5 mol% catalyst loading, their material could yield up to 98% of 1-phenyl-imidazole product with TON of 39.2 (entry 4). Other efficient nanoparticles are a magnetic tethered Cu catalyst that could yield 205 TON with 0.4 mol% catalyst (entry 5).<sup>20</sup> Compared to these copper-based catalysts, the activity of **a-Cu@C** exceeds them at the lowest catalyst loading tested with a TON of 296. This high activity is hypothesized to arise due to the absence of long-range order in **a-Cu@C** and experiments are in progress to obtain this material with higher surface area such that the activities demonstrated here might be further enhanced.

## Conclusions

We have reported a new catalyst system, **a-Cu@C**, obtained from CuNbO-1 pyrolysis for oxidation of benzyl alcohol, reduction of nitrobenzene and N-arylation of imidazole. The TON efficiency for all classes of reactions suggests that there are more active copper sites available on **a-Cu@C**. The yield for the oxidation of benzyl alcohol remained unchanged with a five-times decrease in catalyst loading, and only slightly decreased when 0.5 mol% catalyst was used. The performance of **a-Cu@C** for N-arylation showed a remarkable turnover number with only 0.25 mol% of catalyst. We demonstrate here that the rapid energetic decomposition of CuNbO-1 MOF enabled by strong oxidizing functionality on the MOF linker creates a chemically robust and highly active Cu-carbon composite. Mixed oxidation states allow **a-Cu@C** to function as a general catalyst. Further studies into the active sites, particle size, optimization of the oxidation

## Conflicts of interest

There are no conflicts to declare.

## Acknowledgements

This work was supported by start-up funding from Brigham Young University. This work was also supported by the US Department of Energy [Office of Basic Energy Sciences] DE-FG02-08ER 15997.

## References

- C. M. Friend and B. Xu, *Acc. Chem. Res.*, 2017, **50**, 517-521.
- H. Furukawa, K. E. Cordova, M. O'Keeffe and O. M. Yaghi, *Science*, 2013, **341**, 1230444; A.-L. Li, Q. Gao, J. Xu and X.-H. Bu, *Coord. Chem. Rev.*, 2017, **344**, 54-82; K. K. Gangu, S. Maddila, S. B. Mukkamala and S. B. Jonnalagadda, *Inorg. Chim. Acta*, 2016, **446**, 61-74; R. J. Kuppler, D. J. Timmons, Q.-R. Fang, J.-R. Li, T. A. Makal, M. D. Young, D. Yuan, D. Zhao, W. Zhuang and H.-C. Zhou, *Coord. Chem. Rev.*, 2009, **253**, 3042-3066.
- For current reviews*; K. Shen, X. Chen, J. Chen, and Y. Li, *ACS Catal.*, 2016, **6**, 5887-5903; L. Oar-Arteta, T. Wezendonk, X. Sun, F. Kapteijn and J. Gascon, *Mater. Chem. Front.*, 2017, **1**, 1709-1745; S. Dang, Q.-L. Zhu and Q. Xu, *Nature Reviews*, 2017, **17075**, 1-14. *other examples include*: M. H. Yap, K. L. Fow and G. Z. Chen, *Green Energy Environ.*, 2017, **2**, 218-245; J.-K. Sun and Q. Xu, *Energy Environ. Sci.*, 2014, **7**, 2071-2100; B. Liu, H. Shioyama, T. Akita and Q. Xu, *J. Am. Chem. Soc.*, 2008, **130**, 5390-5391; H.-L. Jiang, B. Liu, Y.-Q. Lan, K. Kuratani, T. Akita, H. Shioyama, F. Zong and Q. Xu, *J. Am. Chem. Soc.*, 2011, **133**, 11854-11857.
- P.-C. Shi, J.-D. Yi, T.-T. Liu, L. Li, L.-J. Zhang, C.-F. Sun, Y.-B. Wang, Y.-B. Huang and R. Cao, *J. Mater. Chem. A*, 2017, **5**, 12322-12329; X.-Q. Wu, J. Zhao, Y.-P. Wu, W.-W. Dong, D.-S. Li, J.-R. Li and Q. Zhang, *ACS Appl. Mater. Interfaces*, 2018, **10**, 12740-12749; D.-D. Zu, L. Lu, X.-Q. Liu, D.-Y. Zhang and L.-B. Sun, *J. Phys. Chem. C*, 2014, **118**, 19910-19917.
- B. R. Kim, J. S. Oh, J. Kim and C. Y. Lee, *Catal. Lett.*, 2016, **146**, 734-743.
- H. Niu, S. Liu, Y. Cai, F. Wu and X. Zhao, *Microporous and Mesoporous Materials*, 2016, **219**, 48-53.
- S. Singha, A. Saha, S. Goswami, S. K. Dey, S. Payra, S. Banerjee, S. Kumar and R. Saha, *Cryst. Growth Des.*, 2018, **18**, 189-199.
- K. A. McDonald, N. Ko, K. Noh, J. C. Bennion, J. Kim and A. J. Matzger, *Chem. Commun.*, 2017, **53**, 7808-7811.
- A. K. Díaz-Duran and F. Roncaroli, *Electrochimica Acta*, 2017, **251**, 638-650.
- M. C. Biesinger, L. W. M. Lau, A. R. Gerson and R. S. C. Smart, *Appl. Surf. Sci.*, 2010, **257**, 887-898; S. Gao, X. Jia, Z. Li and Y. Chen, *J. Nanopart. Res.*, 2012, **14**, 748-758.
- Y. F. Zhang, L. G. Qiu, Y. P. Yuan, Y. J. Zhu, X. Jiang and J. D. Xiao, *Appl. Catal. B Environ.*, 2014, **144**, 863-869.
- J. W. Burrell, S. Gadipelli, J. Ford, J. M. Simmons, W. Zhou and T. Yildirim, *Angew. Chem. Int. Ed.*, 2010, **49**, 8902-8904.
- A. S. Hall, A. Kondo, K. Maeda and T. E. Mallouk, *J. Am. Chem. Soc.*, 2013, **135**, 16276-16279.

- 14 N. Mahmood, C. Zhang, H. Yin and Y. Hou, *J. Mater. Chem. A*, 2014, **2**, 15–32; K. Niu, B. Yang, J. Cui, J. Jin, X. Fu, Q. Zhao and J. Zhang, *J. Power Sources*, 2013, **243**, 65–71; D. A. Bulushev, A. L. Chuvilin, V. I. Sobolev, S. G. Stolyarova, Y. V. Shubin, I. P. Asanov, A. V. Ishchenko, G. Magnani, M. Riccò, A. V. Okotrub and L. G. Bulusheva, *J. Mater. Chem. A*, 2017, **5**, 10574-10583.
- 15 S. Poulston, P. M. Parlett, P. Stone and M. Bowker, *Surface and Interface Analysis*, 1996, **24**, 811-820.
- 16 M. Hudlicky, *Oxidation in organic chemistry*, ACS, Washington, DC, 1990.
- 17 Z. Duan, G. Ma and W. Zhang, *Bull. Korean Chem. Soc.*, 2012, **33(12)**, 4003-4006.
- 18 Z. Jin, *Nat. Prod. Rep.*, 2005, **22**, 196; E. M. Beccalli, G. Broggini, M. Martinelli and S. Sottocornola, *Chem. Rev.*, 2007, **107**, 5318; M. Carril, R. SanMartin and E. Domínguez, *Chem. Soc. Rev.*, 2008, **37**, 639; F. Monnier and M. Taillefer, *Angew. Chem., Int. Ed.*, 2008, **47**, 3096.
- 19 S. K. Movahed, P. Salari, M. Kasmaei, M. Armaghan, M. Dabiri and M. M. Amini, *Appl. Organometal. Chem.*, 2018, **32**, 3914.
- 20 A. R. Sardarian, N. Zohourian-Mashmoul and M. Esmailpour, *Monatsh. Chem.*, 2018, **149**, 1101-1109.